Calculation of the upper critical fields in Nb/Ta multilayers

1996 J. Phys.: Condens. Matter 8 8787

(http://iopscience.iop.org/0953-8984/8/45/014)

J. Phys.: Condens. Matter **8** (1996) 8787–8797. Printed in the UK

Calculation of the upper critical fields in Nb/Ta multilayers

R T W Koperdraad, H T Wu and A Lodder

Faculteit Natuurkunde en Sterrenkunde, Vrije Universiteit, De Boelelaan 1081, 1081 HV Amsterdam, The Netherlands

Received 17 April 1996

Abstract. The Takahashi–Tachiki proximity-effect theory is applied to the Nb/Ta multilayer system. The diffusion coefficients of the two metals and the critical temperature of Nb are used as free parameters in fitting experimental phase diagrams. Magnetic-coherence-length scaling is used in order to obtain phase diagrams that best reproduce the measured data. Several parameter sets can compete in fitting an experimental curve. It is not always possible to decide which set gives the most realistic result.

1. Introduction

After Takahashi and Tachiki [1] launched an advanced theory on upper critical fields in metallic multilayers, only a limited number of authors have studied its implications. Unfortunately, most calculations done with this theory considered model systems only [1–3]. Auvil and Ketterson [4] compared the theory to experiments on Nb/Cu multilayers, but limited themselves to the critical temperature. In their review article, Jin and Ketterson [5] asserted that most systems were still waiting for a thorough analysis in terms of this theory.

In a previous publication [6], we met this demand by extensively studying the V/Ag and Nb/Cu systems. The Takahashi–Tachiki equations were solved exactly and the results were searched for the best possible fits to experimental phase diagrams. As several problems were encountered in obtaining reasonable fits, the analysis of these systems was deepened [7]. A scaling procedure was introduced for the magnetic coherence length, which considerably improved upon the phase diagrams of V/Ag and Nb/Cu, and of the related systems V/Cu and Nb/Ag.

All systems studied previously [4, 6] in the framework of the full Takahashi–Tachiki theory were composed of a superconducting transition metal and a noble metal, the latter being a notorious non-superconductor. For such systems the methods of solution developed by Radović *et al* [8] and Takahashi and Tachiki apply equally well. The present paper aims at a further broadening of the discussion by the analysis of the Nb/Ta multilayer system, in which both metals are superconductors. For such a system the method of Radović *et al* does not work, while the more general eigenfunction method of Takahashi and Tachiki does. Fortunately, Broussard and Geballe [9, 10] provided detailed experimental data for this combination of metals and also Ikebe *et al* [11] did measurements on Nb/Ta. Therefore, an extensive comparison can be made between theory and experiments.

In section 2 the theory [1, 6, 12] and the fitting procedure [6, 7] will be briefly summarized. Section 3 shows the results. The fitting procedure is applied both with and without magnetic-coherence-length scaling. The final section summarizes the conclusions.

0953-8984/96/458787+11$19.50

2. Theory and fitting procedure

The starting point of the Takahashi–Tachiki theory [1, 12] is Gorkov's linearized integral equation for the pair potential [13]

$$\Delta(\boldsymbol{r}) = \int K(\boldsymbol{r}, \boldsymbol{r}')\,\Delta(\boldsymbol{r}')\,\mathrm{d}^3 r'. \tag{1}$$

The kernel $K(\boldsymbol{r}, \boldsymbol{r}')$ can be expanded as

$$K(\boldsymbol{r}, \boldsymbol{r}') = V(\boldsymbol{r}) kT \sum_{\omega} Q_{\omega}(\boldsymbol{r}, \boldsymbol{r}') \tag{2}$$

which contains a position-dependent BCS electron–electron interaction coupling constant $V(\boldsymbol{r})$ and a summation over discrete frequencies $\omega = (2n + 1)\pi kT$. The summation is restricted to frequencies $|\omega| \leqslant \omega_D$, ω_D being the Debye frequency. According to Takahashi and Tachiki, the function $Q_{\omega}(\boldsymbol{r}, \boldsymbol{r}')$ can be derived from the following Green's-function-like differential equation

$$[2|\omega| + L(\boldsymbol{\nabla})] Q_{\omega}(\boldsymbol{r}, \boldsymbol{r}') = 2\pi N(\boldsymbol{r}) \delta(\boldsymbol{r} - \boldsymbol{r}') \tag{3}$$

where $N(\boldsymbol{r})$ is the position-dependent density of states at the Fermi energy. The differential operator $L(\boldsymbol{\nabla})$ is given by

$$L(\boldsymbol{\nabla}) \equiv -\hbar D(\boldsymbol{r}) \left(\boldsymbol{\nabla} - \frac{2\mathrm{i}e\boldsymbol{A}(\boldsymbol{r})}{\hbar c} \right)^2 \tag{4}$$

where $D(\boldsymbol{r})$ is the position-dependent electronic diffusion constant and $\boldsymbol{A}(\boldsymbol{r})$ the vector potential of the applied magnetic field. For multilayers, the three functions $N(\boldsymbol{r})$, $V(\boldsymbol{r})$, and $D(\boldsymbol{r})$ are assumed to be constant within a single material, making discontinuous jumps at the interfaces.

Defining the pair function $F(\boldsymbol{r}) \equiv \Delta(\boldsymbol{r})/V(\boldsymbol{r})$ and expanding $Q_{\omega}(\boldsymbol{r}, \boldsymbol{r}')$ and $F(\boldsymbol{r})$ in terms of the eigenfunctions $\psi_{\lambda}(\boldsymbol{r})$ of the operator $L(\boldsymbol{\nabla})$ with corresponding eigenvalues ϵ_{λ}, the following secular equation is derived:

$$\det \left| \delta_{\lambda\lambda'} - 2\pi kT \sum_{\omega} \frac{1}{2|\omega| + \epsilon_{\lambda}} V_{\lambda\lambda'} \right| = 0 \tag{5}$$

where $V_{\lambda\lambda'}$ is the matrix element $\langle \psi_{\lambda} | V | \psi_{\lambda'} \rangle$. If this equation is satisfied, there are non-trivial solutions for the pair function $F(\boldsymbol{r})$. The highest temperature for which such a solution exists is the field-dependent critical temperature.

For multilayers, the Takahashi–Tachiki theory requires seven input parameters. These are a single (average) value for the Debye temperature and the values for the density of states at the Fermi level N, the normal-state electronic diffusion constant D and the BCS electron–electron coupling constant V for the two constituent metals. Three of these seven properties, the diffusion coefficients of both metals and the density of states of the superconductor (Nb, in the case of Nb/Ta), are used as free parameters to fit three experimental points in the phase diagram: the multilayer critical temperature T_c and the perpendicular and parallel upper critical fields $H_{c2,\perp}(T)$ and $H_{c2,\parallel}(T)$ at a certain temperature T. The fitting procedure generally renders two possible solutions [7], that is, two distinct parameter sets $\{N_{\mathrm{S}}, D_{\mathrm{S}}, D_{\mathrm{N}}\}$ that fit the three points in the phase diagram. The solution with the larger ratio $N_{\mathrm{S}} D_{\mathrm{S}} / N_{\mathrm{N}} D_{\mathrm{N}}$ will be referred to as the first solution. The second solution corresponds to the smaller value of the same ratio.

The $H_{c2,\parallel}$-curves show several characteristic regimes, which depend on the magnitude of the magnetic or Ginzburg–Landau coherence length, $\xi = \sqrt{\hbar c / 2eH}$, in relation to the layer

thicknesses. For the first solutions, the $H_{c2,\parallel}$-curve shows generally two regimes. Close to T_c, where $H_{c2,\parallel}(T)$ is linear, the magnetic coherence length is large and the multilayer behaves as an average bulk material. This is called the average three-dimensional ($\overline{3D}$) regime. At lower temperatures, the curve crosses over to a two-dimensional (2D) regime. Here, the magnetic coherence length is of the order of the layer thicknesses. The pair function nucleates in an S layer and the $H_{c2,\parallel}$-curve shows a square-root-like behaviour. Figure 4—see later—is a typical phase diagram showing these two regimes. For the second solutions, the 2D regime can correspond to nucleation in the N layer. In that case, there can be a third regime at still lower temperatures, where the nucleation point shifts back to the S layer. This is called the three-dimensional (3D) regime. The crossover between 2D and 3D is discontinuous, causing a kink in the $H_{c2,\parallel}(T)$-curve. Figure 5—see later—is phase diagram that shows all three regimes.

By use of a scaling procedure [7], the magnitude of the magnetic coherence length ξ can be controlled independently of the magnetic field H, thus giving much more freedom in fitting the experimental data. The essence of magnetic-coherence-length scaling is the replacement of the original equation with

$$\xi = \sqrt{\frac{\alpha\hbar c}{2eH}} \tag{6}$$

where α is a scaling parameter. Since ξ determines the position of the dimensional crossover in $H_{c2,\parallel}(T)$, scaling uncouples the magnitude of H and the crossover temperature. An external justification is lacking for the introduction of this factor, but it is the only way by which phase diagrams can be modified to represent the data more closely.

3. Results

Broussard and Geballe [9, 10] provided an extensive experimental analysis of the Nb/Ta system. Apart from measuring the phase diagrams, they supplemented their work with the determination of the diffusion coefficients of the separate metals embedded in the multilayer. This was done by measuring the parallel resistivity of the multilayer and separating the contributions of the two metals according to the model of Gurvitch [14]. This offers a nice opportunity to compare the fitting diffusion coefficients to experimental values.

The present system has the advantage that the lattice constants of the two BCC metals are close together. For niobium and tantalum, the values are 3.30 and 3.31 Å, respectively. So the lattices of the metals are not expected to be seriously distorted at the interfaces of this coherent multilayer system. The boundary resistance should be correspondingly low. However, according to Broussard and Geballe [9, 10], the interdiffusion of niobium and tantalum can be an important effect. They state that their sample Nb(1.9 Å)/Ta(1.5 Å) is in fact an anisotropic alloy, rather than a multilayer. For larger layer thicknesses, it might be necessary to account for a NbTa layer in between Nb and Ta. This has, however, not been implemented in the present calculations.

To some extent, Broussard and Geballe gave a theoretical analysis of the experimental results. As far as the critical temperature of thick-layer systems was concerned, they claimed that the results cannot be fitted by the Werthamer theory [9]. The reason they gave is that niobium especially is not in the dirty limit. Therefore, they used a modified version of the Werthamer theory, which is formulated by Kogan [15] and meant to apply to superconductors that are not in the dirty limit. This theory could well reproduce the T_c of the thick-layer systems. For thin-layer systems, only the Cooper–de Gennes limit was calculated. It was stated that a Nb–Ta interface layer of 10 Å is needed to obtain a reasonable correspondence

with the measurements. The perpendicular upper critical fields were examined by using Kogan's theory as well. It was found that the slope of $H_{c2,\perp}(T)$ at T_c could well be described by this theory, but the positive curvature of the curve could not be explained. Parallel upper critical fields were only analysed within the scope of anisotropic Ginzburg–Landau theory. So, Kogan's theory was not used to produce full phase diagrams. In the present work, we do study full diagrams. The Takahashi–Tachiki theory is not restricted to thick-layer systems, nor is it limited to perpendicular magnetic fields. However, it has the restriction that it is valid in the dirty limit only. An extension to less dirty systems is not available.

As before, only the average of the Debye temperatures enters into the theory. We used a value of 267.5 K, which derives from 277 K for Nb and 258 K for Ta. The other fixed parameters, used in applying our fitting procedure, are $N_{\mathrm{Ta}} = N_{\mathrm{Ta(bulk)}} = 8.74 \times 10^{47}$ J^{-1} m^{-3} and V_{Nb} and V_{Ta}. The latter two are determined from the bulk critical temperature and the bulk density of states, using $T_{c,\mathrm{Nb(bulk)}} = 9.26$ K, $N_{\mathrm{Nb(bulk)}} = 11.5 \times 10^{47}$ J^{-1} m^{-3}, $T_{c,\mathrm{Ta(bulk)}} = 4.48$ K and $N_{\mathrm{Ta(bulk)}}$. Now, N_{Nb}, D_{Nb} and D_{Ta} are the free parameters, used to fit the multilayer T_c and the critical fields $H_{c2,\perp}(T)$ and $H_{c2,\parallel}(T)$ for some temperature T to be chosen. Generally, this temperature will be small and correspond to the three-dimensional regime of $H_{c2,\parallel}(T)$. At the end of this section we will also consider fits for which the fit temperature is inside the two-dimensional regime.

Table 1. Fitting parameters of the first solution for Nb/Ta.

$d_{\mathrm{Nb}}/d_{\mathrm{Ta}}$ (Å/Å)	T_c (K)	T_{fit} (K)	$T_{c,\mathrm{Nb}}$ (K)	D_{Nb} (cm^2 s^{-1})	D_{Ta} (cm^2 s^{-1})	$D_{\mathrm{Nb}}^{\mathrm{BG}}$ (cm^2 s^{-1})	$D_{\mathrm{Ta}}^{\mathrm{BG}}$ (cm^2 s^{-1})
1.9/1.5	6.09	4.62	7.28	7.87	0.34	6.6	4.7
10.9/8.6	6.28	4.75	7.61	8.17	0.61	6.7	4.9
18.5/14.5	6.67	4.00	8.28	9.79	1.02	10.2	7.4
30.5/23.9	6.90	3.75	8.67	10.6	1.29	13.8	9.8
52.7/41.4	7.12	3.36	9.04	10.2	1.91	20.5	11.2
89/69	7.29	2.76	9.26	13.7	1.83	31.9	16.6
128/100	7.31	2.25	9.27	15.0	2.39	41.3	16.2
253/199	7.57	3.80	9.54	12.9	3.95	75.5	16.6
98/477	5.57	2.17	9.86	69.1	4.89	164	30
290/490	6.95	3.26	9.21	26.6	2.41	146	24
490/520	7.69	2.40				182	24

3.1. First-solution results

The first-solution results of the above fitting procedure, applied to the data of Broussard and Geballe [9, 10], are listed in table 1. The first three columns show the layer thicknesses, the measured multilayer T_c and the fitting temperature. The fourth to the sixth columns show the fitting material parameters: $T_{c,\mathrm{Nb}}$, D_{Nb} and D_{Ta}. The last two columns show the experimental values of the diffusion coefficients, obtained by Broussard and Geballe from resistivity measurements. The first two rows could be obtained using thin-layer-limit expressions [7, 12]. For the Nb(490 Å)/Ta(520 Å) system, the first solution does not exist. This is due to the combination of relatively thick layers and a relatively small anisotropy at the fitting temperature.

Figure 1 shows the layer-thickness dependence of the niobium critical temperature that results from our fitting procedure. A clear tendency to increase with the layer thickness

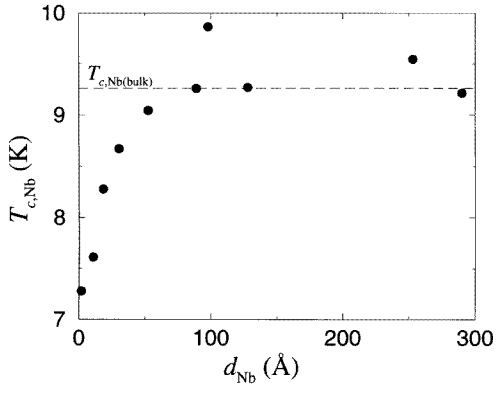

Figure 1. The layer-thickness dependence of the fitting niobium critical temperature, according to the first solution as listed in table 1.

is observed. Apart from the Nb(253 Å)/Ta(199 Å) result, which is slightly too high, and the Nb(98 Å)/Ta(477 Å) result, which is even somewhat higher, the points fall on a single curve. They nicely converge to the bulk niobium T_c, which is indicated by the dashed line. This agrees with the behaviour of a single niobium film [6]. The graph is considerably better than what was found [6] for $T_{c,\mathrm{Nb}}$ in Nb/Cu multilayers.

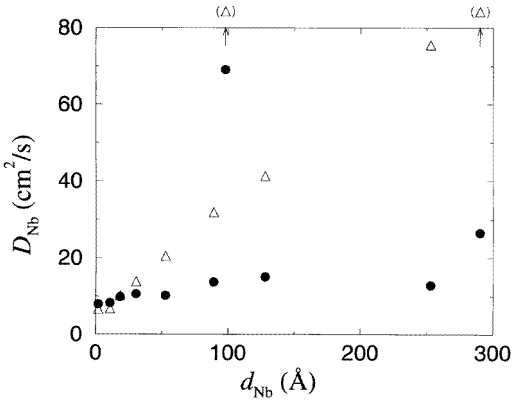

Figure 2. The layer-thickness dependence of the niobium diffusion coefficient as listed in table 1. The solid circles show the first-solution results. The open triangles show the resistivity-measurement-based values of Broussard and Geballe. Two of the data points of Broussard and Geballe are outside the range of this graph. These are indicated by the arrows.

The layer-thickness dependence of the niobium diffusion coefficient is shown in figure 2. The solid circles correspond to the results of the fitting procedure—see the fifth column of table 1. The open triangles represent the measured values of Broussard and Geballe, $D_{\mathrm{Nb}}^{\mathrm{BG}}$—see the seventh column of table 1. There are two deviating values of $D_{\mathrm{Nb}}^{\mathrm{BG}}$ that are outside the range of the graph, namely, the one for Nb(98 Å)/Ta(477 Å) and the one for Nb(290 Å)/Ta(490 Å). Whereas the other values are nicely connected by a single straight line, those two are much higher than can be reconciled with this linear behaviour. From references [9] and [10] it is not clear what this discrepancy arises from. Returning to figure 2, it is seen that at small thicknesses the fitting results coincide with the measurements. But at larger layer thicknesses D_{Nb} does not keep up with the values given by Broussard and Geballe. Although the fitting D_{Nb} increases with the layer thickness, the dependence does not seem to be linear. Again, Nb(98 Å)/Ta(477 Å) is an exception to the general behaviour and falls above all other data points. When comparing the behaviour of figure 2 to the heuristic interface scattering rule of Banerjee *et al* [16] (equation (12) of reference [6]), it is seen that the present results are much larger than predicted by the equation, the difference

being given by a factor of the order 6. According to the information supplied by Broussard and Geballe it seems reasonable to attribute this difference to the fact that the niobium in their Nb/Ta samples is indeed much purer than it is in the Nb/Cu samples [16].

The layer-thickness dependence of the tantalum diffusion coefficient is shown in figure 3. The solid circles correspond to the results of the fitting procedure and the open triangles represent the values of $D_{\mathrm{Nb}}^{\mathrm{BG}}$, as measured by Broussard and Geballe. Again the fitting values increase with the layer thicknesses. At lower temperatures the points can be grouped onto a straight line. At higher temperatures there is a tendency to saturate, but the result for Nb(290 Å)/Ta(490 Å) falls below this general behaviour. For the whole temperature range, the fitting results are much smaller than the values Broussard and Geballe extracted from their resistivity measurements. The overall difference is given by a factor of approximately 5.

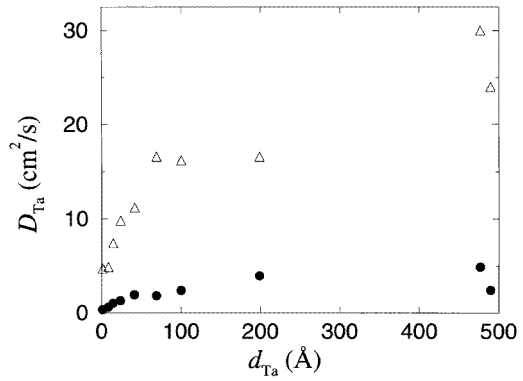

Figure 3. The layer-thickness dependence of the tantalum diffusion coefficient as listed in table 1. The solid circles show the first-solution results. The open triangles show the resistivity-measurement-based values of Broussard and Geballe.

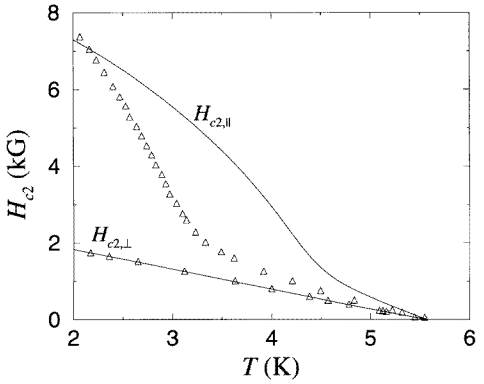

Figure 4. The upper-critical-field curves of Nb(98 Å)/Ta(477 Å). The first solution is shown. The triangles show the data points of Broussard and Geballe (references [9, 10]).

Using the fitting parameters of table 1 we can calculate the critical fields over the whole temperature domain and compare them to the experimental points. The phase diagrams of the systems with $d_{\mathrm{Ta}} \leqslant 100$ Å show an average three-dimensional ($\overline{3\mathrm{D}}$) behaviour at all temperatures. Since there is no dimensional crossover for these systems, the calculated curves can easily reproduce the experimental ones. The curves in this regime are linear. The three remaining systems show a dimensional crossover from average three-dimensional to two-dimensional (2D) behaviour. Figure 4 is an example of such a system, namely, Nb(98 Å)/Ta(477 Å). The solid lines are the theoretical curves, which have been fitted to the data at 2.17 K. The triangles show the measured data [9]. The measured $H_{c2,\perp}$ is almost linear,

in contrast to the results for Nb/Cu, where a positive curvature was found. Since a linear temperature dependence can easily be fitted by the first solution, the perpendicular upper critical field is very well reproduced by the theory. The experimental $H_{c2,\parallel}$ exhibits a single smooth dimensional crossover, that looks qualitatively the same as the crossovers observed in Nb/Cu. The crossover temperature T^* (the point of maximum curvature) is measured at 3.1 K. It is seen that the calculated curve has a dimensional crossover of the same kind, but at a higher temperature, namely, $T^* = 4.44$ K. This and the overestimation of the anisotropy near T_c cause an overestimation of the parallel upper critical field everywhere above the fitting temperature. A better result can be obtained by using a scaled magnetic coherence length, as in equation (6), with a scaling factor of $\alpha = 2$. The scaled fitting material parameters are $T_{c,\mathrm{Nb}} = 10.12$ K, $D_{\mathrm{Nb}} = 141$ cm^2 s^{-1} and $D_{\mathrm{Ta}} = 8.25$ cm^2 s^{-1}. The diffusion coefficients are approximately a factor of α larger. They are closer to, but still smaller than the resistivity-measurement-based values given by Broussard and Geballe. The niobium critical temperature has increased with respect to the unscaled solution. Its value exceeds the bulk niobium T_c by 0.9 K. As a result of the scaling T^* has shifted to 3.56 K. However, scaling does not improve upon the high-temperature anisotropy. Consequently, the resulting curve for $H_{c2,\parallel}$ still overestimates the experimental results.

Table 2. Fitting parameters of the second solution for Nb/Ta.

$d_{\mathrm{Nb}}/d_{\mathrm{Ta}}$ (Å/Å)	T_c (K)	T_{fit} (K)	$T_{c,\mathrm{Nb}}$ (K)	D_{Nb} (cm^2 s^{-1})	D_{Ta} (cm^2 s^{-1})	$D_{\mathrm{Nb}}^{\mathrm{BG}}$ (cm^2 s^{-1})	$D_{\mathrm{Ta}}^{\mathrm{BG}}$ (cm^2 s^{-1})
1.9/1.5	6.09	4.62	7.28	0.34	12.1	6.6	4.7
10.9/8.6	6.28	4.75	7.61	0.60	12.6	6.7	4.9
18.5/14.5	6.67	4.00	8.28	0.98	15.4	10.2	7.4
30.5/23.9	6.90	3.75	8.67	1.21	16.8	13.8	9.8
52.7/41.4	7.12	3.36	9.04	1.73	16.2	20.5	11.2
89/69	7.29	2.76	9.26	1.63	23.5	31.9	16.6
128/100	7.31	2.25	9.22	1.37	29.4	41.3	16.2
253/199	7.57	3.80	9.15	0.97	198	75.5	16.6
98/477	5.57	2.17	8.20	0.15	956	164	30
290/490	6.95	3.26	9.26	1.38	238	146	24
490/520	7.69	2.40	9.76	4.29	116	182	24

3.2. Second-solution results

The results of the second type of solution are listed in table 2. From the left to the right, the successive columns show the layer thicknesses, the multilayer T_c, the fitting temperature, the fitting $T_{c,\mathrm{Nb}}$, D_{Nb} and D_{Ta} and the measured values of the diffusion coefficients, obtained by Broussard and Geballe from resistivity measurements.

For the three-dimensional multilayers ($d_{\mathrm{Ta}} \leqslant 100$ Å), the fitting values of $T_{c,\mathrm{Nb}}$ are almost the same as for the first solution. The points fall on a single curve. A tendency to increase with the niobium layer thickness is observed and at $d_{\mathrm{Nb}} = 89$ Å the value of $T_{c,\mathrm{Nb}}$ has converged to the bulk T_c. The four two-dimensional multilayers show a tendency of their own, that cannot be reconciled with the behaviour of the thin-layer systems. The corresponding values of $T_{c,\mathrm{Nb}}$ again fall on a single curve, that neatly increases with the layer thickness. But this curve is clearly not an extrapolation of the thin-layer results and it continues to increase after the bulk niobium T_c has been reached.

The values found for D_{Nb} are much smaller than was found for the first solution. It

is impossible to extract a tendency from its behaviour with the layer thickness. Even the fact that the diffusion coefficients should be larger for thicker layers is not supported by the data. The lack of cohesion of D_{Nb} as a function of layer thickness strongly suggests that the first solution is a much better alternative.

For the second-solution results for the fitting tantalum diffusion coefficient, there is again a clear distinction between the thin- and the thick-layer behaviour. For $d_{\mathrm{Ta}} \leqslant 100$ Å, the layer-thickness dependence is approximately linear and the fitting values increase with the layer thickness. The deviation from the values of Broussard and Geballe is close to 6 cm^2 s^{-1} for all of these multilayers. For thick-layer systems, however, extreme values for D_{Ta} are found, that do not fit in with any cohesive behaviour. This provides us with another reason to set a higher value upon the first solution.

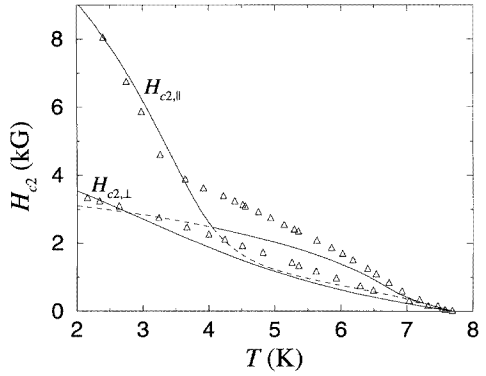

Figure 5. The upper-critical-field curves of Nb(490 Å)/Ta(520 Å). The graph shows the second solution without magnetic-coherence-length scaling. The triangles show the data points of Broussard and Geballe (reference [9]).

Due to the extreme ratios found between the fitting diffusion coefficients of the two-dimensional systems, the corresponding calculated phase diagrams have extreme characteristics. Figure 5 illustrates this for the Nb(490 Å)/Ta(520 Å) system. The perpendicular upper critical field shows a very strong positive curvature. This is in disharmony with the experimental findings, represented by the open triangles. For the parallel upper critical field, the correspondence is much better. There is a large temperature region, ranging from 4 to 7 K, where nucleation occurs in the Ta layer. At 4.05 K, there is a discontinuous dimensional crossover, to the left of which the calculated curve fits the experimental data. Remarkably, the crossover looks very similar to the one that was actually measured, although it has a different position in the H–T plane. Actually, the measured $H_{c2,\parallel}$ suggest that nucleation in the Ta layer really takes place. However, the large region of nucleation in Ta is due to the large ratio of the diffusion coefficients of the metals. It was precisely this large ratio that caused the positive curvature of $H_{c2,\perp}$. Therefore, the implication of the measured $H_{c2,\perp}$ is that such a large ratio does not exist and, consequently, that nucleation in tantalum is highly improbable.

3.3. The Nb(490 Å)/Ta(520 Å) system

It is interesting to dwell upon the phase diagram of Nb(490 Å)/Ta(520 Å). It was found, using a fitting temperature of 2.40 K, that the first solution did not exist. This problem may well be overcome by using another fitting temperature. Since 2.40 K was in the three-dimensional regime, one might try to use a temperature located in the 2D regime. When using 4.22 K, a first solution does indeed exist. It leads to a niobium critical temperature of 10.05 K and the fitting diffusion coefficients are $D_{\mathrm{Nb}} = 16.3$ cm^2 s^{-1} and

$D_{\mathrm{Ta}} = 13.5$ cm^2 s^{-1}. The phase diagram, corresponding to these parameters, is depicted in figure 6. The result for $H_{c2,\parallel}$ is remarkable. Although the three-dimensional regime is missing completely from the curve, both the 2D and the $\overline{\mathrm{3D}}$ regimes are fitted perfectly. Apparently, the high-temperature behaviour can well be described by moderate diffusion coefficients and nucleation in Nb. The $H_{c2,\perp}$-curve deviates somewhat, showing a slightly overestimated concavity.

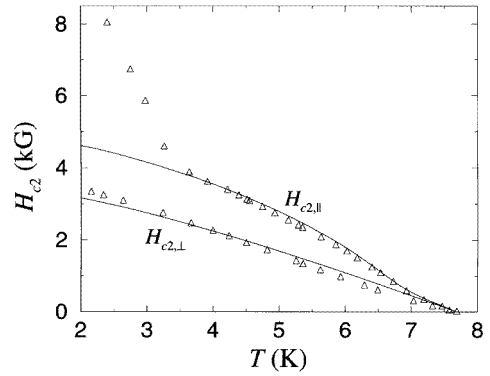

Figure 6. The upper-critical-field curves of Nb(490 Å)/Ta(520 Å). The graph shows the first solution, obtained by fitting the critical fields at a temperature in the two-dimensional regime. The triangles show the data points of Broussard and Geballe (reference [9]).

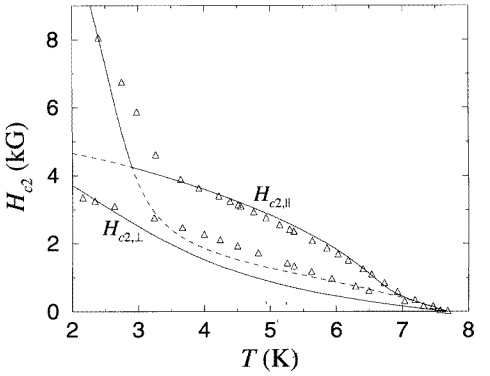

Figure 7. The upper-critical-field curves of Nb(490 Å)/Ta(520 Å). The graph shows the second solution. A scaling factor $\alpha = 2$ has been used for the magnetic coherence length. The triangles show the data points of Broussard and Geballe (reference [9]).

An amazing result is obtained by applying magnetic-coherence-length scaling, equation (6), to the second solution (see figure 5). When using $\alpha = 2$ and a fitting temperature of 1.5 K, we find the fitting material parameters $T_{c,\mathrm{Nb}} = 9.84$ K, $D_{\mathrm{Nb}} = 4.64$ cm^2 s^{-1} and $D_{\mathrm{Ta}} = 328$ cm^2 s^{-1}. The corresponding phase diagram is shown in figure 7. Again, we find a curve that fits the two-dimensional and the 3D-average regime of $H_{c2,\parallel}$ perfectly. In fact, on the right-hand side of the kink ($T > 2.91$ K), the curve coincides with the first-solution diagram of figure 6. So the high-temperature behaviour can also be described by extreme diffusion coefficients and nucleation in Ta. Clearly, when comparing figures 6 and 7, the former reproduces the measured perpendicular upper critical field much better. On the other hand, the latter has a 3D regime that, indeed, does not coincide with the measured curve, but that is at least of the same character as the experimental low-temperature regime. The theory does not give a decisive answer to the question of the real nucleation point. On the one hand, the shape of the two-dimensional regime seems to allow for both possibilities. On the other hand, the three-dimensional regime and $H_{c2,\perp}$ suggest opposite possibilities.

3.4. The fitting to the data of Ikebe et al

Ikebe *et al* [11] also measured the upper critical fields of Nb/Ta. Only a single multilayer was studied, with layer thicknesses of 100 Å for both metals. The sample used is of a very different nature to the ones used by Broussard and Geballe. The upper critical fields are almost a factor of 5 larger. Since H_{c2} is roughly inversely proportional to the diffusion coefficients, this implies that the samples of Ikebe *et al* are much more dirty. The fitting material parameters of the first solution are $T_{c,\mathrm{Nb}} = 6.57$ K, $D_{\mathrm{Nb}} = 2.80$ cm^2 s^{-1} and $D_{\mathrm{Ta}} = 0.737$ cm^2 s^{-1}. The latter two values are much smaller than the values mentioned in table 1, due to the dirtiness of the present sample. The niobium T_c is remarkably low, which may well be a side-effect of the small diffusion coefficients. Concerning the phase diagram of this system, $H_{c2,\perp}$ is fitted perfectly by the calculated curve. However, the experimental graph of $H_{c2,\parallel}$ is linear, whereas the calculated one has a positive curvature and a weak dimensional crossover. Since the latter is only vaguely present, the overall correspondence of the theory and the measurements is not too much disturbed by this disagreement.

4. Conclusions

We have computed exact solutions of the Takahashi–Tachiki equation and compared them to experiments. An earlier discussion was extended to another combination of metals into multilayers, namely, Nb/Ta, in which both metals are superconductors. For this system, the amount of data available is rather complete. It was found that the fitting material parameters of the first solution were in good agreement with the expectations, although the diffusion coefficients determined from resistivity measurements did not always match with the fitting results. For Nb(490 Å)/Ta(520 Å), the experimental phase diagram suggested that the first solution with T_{fit} in the 2D regime was preferable as far as perpendicular fields were considered, but only the second solution could reproduce the parallel upper critical field to a reasonable extent. When only the high-temperature part of the phase diagram was considered, the parallel upper critical field could be fitted by both the first and the second solutions, with nucleation in Nb and Ta, respectively. It is remarkable that these two very different types of solution can nevertheless yield an identical high-temperature behaviour.

Presumably, the agreement between theory and experiment will be better when a less dirty version of the theory is used. The tentative theoretical analysis of Nb/Ta by Broussard and Geballe points in that direction. Currently, such a modified version is only available in the Werthamer approximation. The corresponding modification of the Takahashi–Tachiki theory is a subject of future research.

Acknowledgments

We would like to thank P R Broussard for supplying us with the files of experimental data. This work is part of the research programme of the Stichting voor Fundamenteel Onderzoek der Materie (FOM), which is financially supported by the Nederlandse Organisatie voor Wetenschappelijk Onderzoek (NWO).

References

[1] Takahashi S and Tachiki M 1986 *Phys. Rev.* B **33** 4620
[2] Takahashi S and Tachiki M 1986 *Phys. Rev.* B **34** 3162
[3] Takanaka K 1991 *J. Phys. Soc. Japan* **60** 1070

[4] Auvil P R and Ketterson J B 1988 *Solid State Commun.* **67** 1003
[5] Jin B Y and Ketterson J B 1989 *Adv. Phys.* **38** 189
[6] Koperdraad R T W and Lodder A 1995 *Phys. Rev.* B **51** 9026
[7] Koperdraad R T W and Lodder A 1996 *Phys. Rev.* B **54** 515
[8] Radović Z, Ledvij M and Dobrosavljević-Grujić L 1991 *Phys. Rev.* B **43** 8613
[9] Broussard P R and Geballe T H 1987 *Phys. Rev.* B **35** 1664
[10] Broussard P R and Geballe T H 1988 *Phys. Rev.* B **37** 60
[11] Ikebe M, Obi Y, Kamiguchi Y, Fukumoto Y, Nakajima H, Muto Y and Fujimori H 1987 *Japan. J. Appl. Phys.* **26** 1447
[12] Lodder A and Koperdraad R T W 1993 *Physica* C **212** 81
[13] Gorkov L P 1960 *Sov. Phys.–JETP* **10** 998
[14] Gurvitch M 1986 *Phys. Rev.* B **34** 540
[15] Kogan V 1985 *Phys. Rev.* B **32** 139
[16] Banerjee I, Yang Q S, Falco C M and Schuller I K 1982 *Solid State Commun.* **41** 805